06.1

# Electrochemical performance of LIB anodes based on silicon monoxide: the effect of disproportionation and treatment in HF

© A.A. Grushina[1,2], D.A. Lozhkina[2], A.A. Krasilin[2], A.M. Rumyantsev[2], E.V. Astrova[2]

[1] St. Petersburg State Institute of Technology Institute (Technical University), St. Petersburg, Russia
[2] Ioffe Institute, St. Petersburg, Russia
E-mail: darina.lozhka94@gmail.com

*Received October 13, 2022*
*Revised October 13, 2022*
*Accepted December 22, 2022*

Composite SiO/C anodes for lithium-ion batteries (LIB) obtained by carbonization of silicon monoxide with fluorocarbon were investigated. Preliminary modification of the initial silicon monoxide was carried out by disproportionation and subsequent treatment in hydrofluoric acid. The study of the elemental composition of modified SiO and the electrochemical performance of composite anodes made from it showed that the oxygen content in the oxide matrix played a decisive role in changing their behavior. Depletion of it with oxygen as a result of treatment in HF had a beneficial effect, leading to higher stability of the electrodes during cycling, an increase in their capacity, coulombic efficiency and rate capability.

**Keywords:** composite SiO/C anodes, lithium-ion batteries, treatment in HF.

DOI: 10.21883/TPL.2023.03.55674.19392

Silicon oxides are regarded as anodic materials alternative to silicon in lithium-ion batteries, since they offer a high charge transfer rate and a less pronounced variation of capacity during cycling. However, the high resistance of SiO anodes makes them less electrochemically active, and the production of irreversible phases within the first cycle leads to a relatively low initial Coulombic efficiency. Different ways to solve these problems, such as the production of various composites and disproportionation (DP) [1], have been proposed. DP is the decomposition of SiO in the process of high-temperature annealing with the precipitation of a new phase of nanocrystalline silicon embedded into a dielectric dioxide matrix [2].

The material produced this way is hereinafter denoted as *d*-SiO. Dependences of the amount of produced Si, the size of its precipitates, and the composition of the matrix surrounding these precipitates on the annealing temperature were examined by quantitative X-ray diffraction analysis [3]. The method of carbonization, which relies on interaction with solid-phase fluorocarbon at a relatively low temperature (600−800°C) [4–6], was proven efficient in the synthesis of SiO/C and *d*-SiO/C composites. It was found in [4,7] that the capacity parameters of anodes made of *d*-SiO/C composites improve considerably when the oxide content in *d*-SiO/C decreases. In the present study, we examine this effect by performing preliminary modification of SiO: subjecting it to high-temperature DP and processing in hydrofluoric acid.

The electrode material was synthesized in stages. At the first stage, the initial powder of high-purity silicon monoxide was annealed at 1200°C in high-purity argon for 1 h to produce *d*-SiO. The initial SiO and *d*-SiO were then etched in a 24 wt.% solution of hydrofluoric acid for 15 min at room temperature. This was followed by evaporation of the solution (10 min at $T \approx 70$°C). SiO−HF and *d*-SiO−HF powders were obtained after etching. The elemental composition of powders before and after etching was determined by energy-dispersive X-ray spectroscopy (EDS) using a FEI Quanta 200 electron microscope. At the second stage, all four materials (initial SiO, *d*-SiO, SiO−HF, and *d*-SiO−HF) were subjected to carbonization with fluorocarbon. Each powder was mixed with fluorocarbon $CF_{0.8}$ (Halo Polymer) in a 40:60 wt.% proportion and ground in an agate mortar for this purpose. Pellets 10 mm in diameter and $\sim 650\,\mu$m and thickness were formed from the obtained mixture by cold dry pressing under a pressure of 180 MPa and annealed in Ar in a quasi-closed volume of graphite assemblies at $T = 800$°C for 20 min. The heating rate was 3.3°C/min. Note that $T = 800$°C is certainly below the onset temperature of SiO disproportionation, which becomes apparent only at $T > 900$°C. The thickness of pellets was reduced to $\sim 110\,\mu$m by polishing to prepare them for electrode fabrication. The obtained samples were then glued to copper foil with a suspended mixture of polyvinylidenfluoride, highly exfoliated graphite, and N-methyl-2-pyrrolidone. Two-electrode CR2032 cells with a lithium counter electrode were used for electrochemical studies. Tinci TC-E918, which is a 1 M solution of $LiPF_6$ in an EC/PC/DEC/EMC/PA mixture (ethylene carbonate, propylene carbonate, diethyl carbonate, ethyl methyl carbonate, propyl acetate), was used as an electrolyte. Galvanostatic measurements were performed using a CT-3008W-5V10mA (Neware) battery testing system. The anode voltage in charging (lithiation) and discharging (delithiation) was limited to 10 mV and 2 V, respectively. The charging and discharging current densities were 10 and 20 mA/g.

**Table 1.** Elemental composition of samples

| Sample number | Sample | Si, at.% | O, at.% | F, at.% | $y = [O]/[Si]$ (effective composition $SiO_y$) | $x$ in the $SiO_x$ matrix |
|---|---|---|---|---|---|---|
| 1 | SiO | 54.22 | 45.78 | 0 | 0.84 | 0.84 |
| 2 | SiO–HF | 55.67 | 41.36 | 2.97 | 0.74 | 0.74 |
| 3 | *d*-SiO | 53.40 | 46.60 | 0 | 0.87 | 1.74 |
| 4 | *d*-SiO–HF | 72.69 | 25.54 | 1.77 | 0.35 | 0.70 |

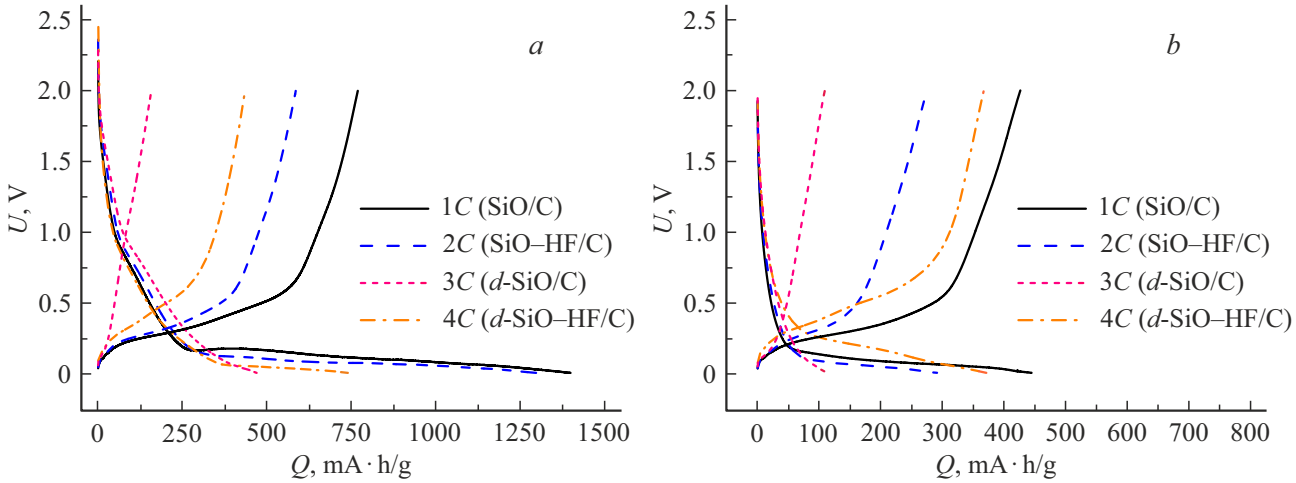


**Figure 1.** Charging-discharging curves of cycles 1 (*a*) and 10 (*b*).

EDS data for powders studied prior to carbonization are listed in Table 1. These data demonstrate that the initial powder is nonstoichiometric silicon monoxide depleted in oxygen ($y = 0.84$). In the general case, the DP reaction is written as

$$2SiO_y \rightarrow f\,Si + Si_{(2-f)}O_{2y}, \qquad (1)$$

where $f$ is the number of precipitate silicon atoms. Let us denote the averaged composition of the amorphous matrix surrounding Si precipitates in *d*-SiO as $SiO_x$. The two-phase powder produced as a result of DP may be characterized by effective composition $SiO_y$, where $y = [O]/[Si]$ is the ratio of oxygen and silicon concentrations (in at.%). It follows from (1) that $SiO_x = Si_{(2-f)}O_{2y}$ or $x = y/(1 - f/2)$. It was demonstrated in [3] that complete disproportionation with $f = 1$ (and, consequently, $x = 2y$) occurs at a temperature of 1200°C. DP of the initial $SiO_{0.9}$ monoxide did indeed result in the formation of oxide matrix $SiO_{1.8}$, and the size of Si precipitates was 13.4 nm.

Let us return to Table 1. It is evident that the values of $y$ before and after DP (in samples Nos. 1 and 3) should be the same. However, this value for sample No. 3 is somewhat higher ($y = 0.87$), which is apparently attributable to partial oxidation of Si in the process of annealing. In accordance with (1), $x = 1.74$ for the matrix of sample No. 3. This value agrees fairly well with the data from [3] (see above). Following treatment in hydrofluoric acid, fluorine from residual reaction products is introduced into the composition of powders, and the value of $y$ decreases (in sample No. 4 this reduction is greater than in sample No. 2). It is known that the rate of etching in HF increases by several orders of magnitude in the Si→SiO→$SiO_2$ sequence. Thus, oxides with the greatest amount of oxygen dissolve first, and oxides of exactly this kind form as a result of high-temperature SiO DP. It should be noted that the values of $x$ characterizing the matrix composition in samples Nos. 2 and 4 are close (0.74 and 0.70, respectively). Since hydrofluoric acid has almost no effect on silicon at room temperature, silicon oxides with approximately the same averaged composition are left in these two samples after etching. Figure 1, *a* presents the charging-discharging curves of cycle 1 for composite anodes Nos. 1*C*–4*C* fabricated from the corresponding powders Nos. 1–4 (Tables 1 and 2). These plots demonstrate that the charging curve of samples Nos. 1*C* and 2*C* has an extended plateau, which is typical of lithium insertion into SiO. This plateau vanishes after DP in sample No. 3*C*, and the capacity decreases significantly. HF processing, which followed after DP, again induced an increase in capacity, and the plateau was restored (sample No. 4*C*). Charging-discharging curves in Fig. 1 demonstrate that the charge and discharge capacities of the initial silicon monoxide etched in HF decrease, while the same parameters of *d*-SiO increase after etching. It follows from Table 2 that $Q_{dch}$ of composite No. 2*C* fabricated from the initial SiO processed in hydrofluoric acid is lower

**Table 2.** The values of charge and discharge capacities, Coulombic efficiency at cycle 1, fraction of the discharge capacity retained at cycle 10, and capacity drop at cycle 11 induced by the growth of current from 10 to 20 mA/g

| Sample number | Sample | $Q_{ch}$, mA · h/g | $Q_{dch}$, mA · h/g | CE, % | $Q_{10}/Q_1$, % | $\Delta Q_{20\,\mathrm{mA/g}}/Q_{10\,\mathrm{mA/g}}$, % |
|---|---|---|---|---|---|---|
| 1*C* | SiO/C | 1399.8 | 769.4 | 55 | 55.4 | 21.7 |
| 2*C* | SiO–HF/C | 1297.9 | 585.8 | 45.1 | 47.0 | 38.7 |
| 3*C* | *d*-SiO/C | 469.6 | 157.7 | 33.6 | 71.8 | – |
| 4*C* | *d*-SiO–HF/C | 740 | 435.1 | 58.8 | 84.4 | 14.9 |

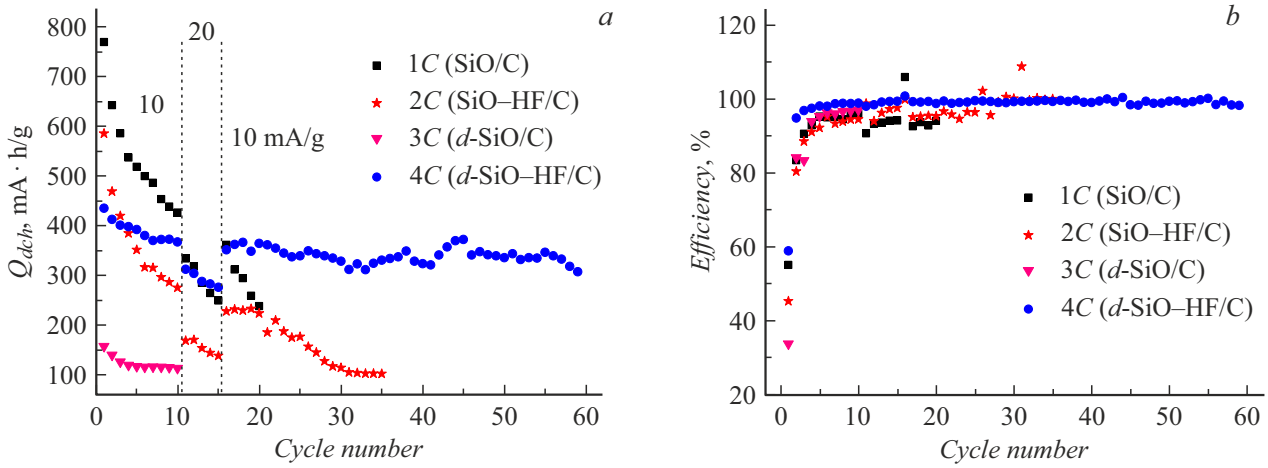


**Figure 2.** Dependence of the discharge capacity ($a$) and the Coulombic efficiency ($b$) on the cycle number.

than the corresponding parameter of the unetched sample, while the etching of *d*-SiO (composite No. 4*C*) induces a $\sim 2.8$ times increase of discharge capacity. The Coulombic efficiency also increases by a factor of $\sim 1.8$. The discharge capacity for all electrodes decreases gradually in the process of further cycling (Figs. $1, b$, $2, a$). However, the highest stability is demonstrated by electrode No. 4*C*, which reaches a constant capacity level of 84.4% of the initial capacity at cycle 10; the capacity at cycle 10 ($Q_{10}/Q_1$) for samples No. 1*C* and 2*C* based on SiO decreases by a factor of 2 (Table 2). Sample No. 4*C* also differs from the other samples in that it reaches a high Coulombic efficiency in a fewer number of cycles (Fig. $2, b$). The increase in current density after cycle 10 induces a capacity reduction $\Delta Q_{20\,\mathrm{mA/g}}/Q_{10\,\mathrm{mA/g}} = (Q_{10\,\mathrm{mA/g}} - Q_{20\,\mathrm{mA/g}})/Q_{10\,\mathrm{mA/g}}$ (Table 2), which is the least pronounced (14.9%) for sample No. 4*C*. When the earlier 10 mA/g regime is restored at cycle 16, the capacity of all samples increases. In the case of sample No. 4*C*, the capacity almost reaches the level determined before the current rise and stays at this level in subsequent cycling, while samples Nos. 1*C* and 2*C* degrade rapidly. Sample No. 3*C* was pulled out of tests due to a low capacity ($\sim 100$ mA · h/g).

Anode materials based on silicon monoxide are conversion-type materials with an irreversible reaction of production of silicon, lithium oxide, and lithium silicates [1] proceeding in them during the first lithiation. This is the reason why the Coulombic efficiency of cycle 1 is lower than the one for silicon electrodes. Reversible recharging in subsequent cycles then proceeds via lithiation and delithiation of the produced silicon:

$$\mathrm{Si} + x\mathrm{Li}^+ + xe^- \leftrightarrow \mathrm{Li}_x\mathrm{Si}. \qquad (2)$$

However, silicon nanoparticles may be produced before lithiation as a result of DP. The size, structure, and amount of Si precipitates in this case may differ from the parameters of precipitates produced at cycle 1 as a result of irreversible interactions between lithium and SiO [1]. However, variations of composition and structure of the $SiO_x$ matrix in the process of DP under high-temperature annealing and/or in the process of etching in HF are the key factor shaping the behavior of electrodes. DP leads to an increase in $x$, while HF processing suppresses it. The process of etching in HF reduces the fraction of oxides with a high oxygen concentration in the shell around silicon particles and enhances their porosity. The matrix then becomes more permeable for the electrolyte and lithium ions, thus facilitating their interaction with Si particles. An increase in the Si phase amount and the size of Si particles and a reduction in the fraction of oxides also contribute to an increase in the Coulombic efficier due to a decrease in irreversible losses caused by the formation of lithium silicates and $Li_2O$. of lithium silicates and $Li_2O$. The electrode lithiation potential decreases (Fig. $1, a$) as $x$

grows in the material after DP. Hence, the electrode ceases to charge, since the lithiation voltage quickly reaches the set limit of 10 mV. The lithiation potential increases after HF processing of this material, and the electrode capacity increases accordingly.

Thus, the electrochemical characteristics and the stability of operation of SiO-based electrodes depend on the presence of crystalline silicon particles in SiO and the permeability of the oxide shell of these particles for $Li^+$ ions. This permeability, in turn, depends on the concentration of oxygen in the shell. These parameters may be adjusted by performing DP and etching in HF. The best results of material modification are achieved by combining DP with subsequent HF treatment. The first process induces the formation of silicon nanoparticles, and the second one reduces the concentration of oxygen in the oxide matrix.

### Acknowledgments

The authors wish to thank V.P. Ulin for helpful discussions.

### Funding

This study was carried out under the state assignment, project 0040-2019-0012.

### Conflict of interest

The authors declare that they have no conflict of interest.

## References

[1] Zh. Liu, Q. Yu, Y. Zhao, R. He, M. Xu, S. Feng, S. Li, L. Zhou, L. Mai, Chem. Soc. Rev., **48** (1), 285 (2019). DOI: 10.1039/C8CS00441B
[2] M. Mamiya, M. Kikuchi, H. Takei, J. Cryst. Growth, **237** (3), 1909 (2002). DOI: 10.1016/S0022-0248(01)02244-8
[3] D.A. Lozhkina, E.V. Astrova, R.V. Sokolov, D.A. Kirilenko, A.A. Levin, A.V. Parfeneva, V.P. Ulin, Semiconductors, **55** (4), 423 (2021). DOI: 10.1134/S1063782621040096.
[4] D.A. Lozhkina, E.V. Astrova, A.M. Rumyantsev, Tech. Phys., **92** (3), 339 (2022). DOI: 10.21883/TP.2022.03.53264.267-21.
[5] E.V. Astrova, V.P. Ulin, A.V. Parfeneva, A.V. Nashchekin, V.N. Nevedomskiy, M.V. Baidakova, Semiconductors, **54** (8), 900 (2020). DOI: 10.1134/S1063782620080059.
[6] D.A. Lozhkina, E.V. Astrova, A.I. Likhachev, A.V. Parfeneva, A.M. Rumyantsev, A.N. Smirnov, V.P. Ulin, Tech. Phys., **66**, 1228 (2021). DOI: 10.1134/S1063784221090103.
[7] J. Yang, Y. Takeda, N. Imanishi, C. Capiglia, J.Y. Xie, O. Yamamoto, Solid State Ion., **152-153**, 125 (2002). DOI: 10.1016/S0167-2738(02)00362-4